Yellowtail Flounder Larval Habitat Suitability of the Northeast U.S. Continental Shelf

M. Conor McManus[1], David E. Richardson[1]
[1]NOAA NMFS Northeast Fisheries Science Center, Narragansett, RI 02882

Abstract

Ichthyoplankton monitoring programs provide insight into the life history and population dynamics of marine species. These fisheries-independent surveys can be useful in understanding the life cycle processes and population bottlenecks between spawner to recruit life stages. Within the Northeast U.S. Shelf ecosystem, adult and juvenile abundances for many fish and invertebrates have shifted over time, often concurrent with changes in the environment. For larval fish, however, there are far fewer examples of exploring the correspondence between larval abundance and distribution with oceanography. We developed larval habitat suitability models for three yellowtail flounder (*Limanda ferruginea*) U.S. stocks (Southern New England-Mid Atlantic, Georges Bank, Cape Cod-Gulf of Maine). Habitat suitability models were constructed to determine how environmental variables correspond to larval abundance. Model predictions were then use to index how habitat suitability for yellowtail flounder within the stock units has changed over time. Several environmental variables were found to correspond to larval abundance, including sea temperature, copepod abundance and climate oscillations. When calculating habitat suitability indices for the stocks, their trajectories were similar over time: increasing habitat suitability in the 1970s and 1980s, and declining in the 2000s. Constructed larval indices for the Southern New England-Mid Atlantic (SNEMA) stock were compared to the stock's habitat suitability to determine whether changes in habitat have induced variability in the stock's larval production. Larval abundance and habitat suitability were significantly, but weakly, correlated. The weak correlation suggests that environmental habitat conditions for the SNEMA stock may not be the greatest determinant in larval production. This work serves as an example of identifying environmental drivers in early life stage fish.

Key Words: habitat suitability, larvae, yellowtail flounder

Introduction

Long-term fisheries surveys monitoring early-life stages allow for understanding population connectivity and life cycle dynamics for marine fish. Such ichthyoplankton survey data can be used for several applications, such as estimating spawning stock biomass, describing spawning or larval habitat preferences, understanding planktonic food web ecology, discerning environmental drivers of fish stocks, and understanding recruitment variability.

Larval survival can be driven by varying environmental conditions, including temperature, salinity, acidification, planktonic food availability, circulation, and predators. Under a changing climate, many of these oceanographic properties have shifted, ultimately altering the habitat available to marine fish, which can vary by species and life stage. Changes in larval fish abundance and distribution have changed within the U.S. Atlantic shelf (Walsh et al. 2015), with ties to changes in the oceanographic environment identified for several species or larval communities (McManus et al. 2018; Morson et al. 2019; Taxton et al. 2020; McManus et al. 2022; Weisberg et al. 2024).

Yellowtail flounder (*Limanda ferruginea*) are a flatfish distributed throughout the Northeast U.S. Shelf Ecosystem (hereafter NEUS), with a long history of reported environmental correlates to population dynamics (Kittel et al. 2024). Currently in U.S. waters, the species is managed as three unique stock units based on varying biological and life history characteristics: Southern New England/Mid-Atlantic (SNEMA), Georges Bank (GB), and Cape Cod/Gulf of Maine (CCGOM). Larval abundances and distribution have been monitored over time in this region, which has indicated that larval yellowtail flounder abundances have shifted northward over the last several decades (Walsh et al. 2015). However, the environmental drivers on this component of the life cycle have not been explored.

Here, we aimed to better understand the environmental drivers in larval yellowtail flounder abundance and distribution within the NEUS. First, larval abundance was evaluated in the context of field, oceanographic, and climate data to understand the conditions in which larvae are present, with models serving as a tool for discerning suitable larval habitat. With these habitat suitability models, we then created spatial predictions of larval abundance to derive stock-specific larval habitat indices and infer how suitable habitat has changed over time. In doing so, we provided insight on what variables and conditions are important for yellowtail flounder larvae, and a quantitative index for use either in stock assessment modeling or informing assessment modeling decisions for the yellowtail flounder stocks.

Methods

Survey

Ichthyoplankton, zooplankton, and oceanographic data have been collected over the last five decades in the NEUS through various long-term monitoring programs

(Kane, 2003; Richardson et al. 2010). Data used in this study were derived from two programs conducted by the National Oceanic and Atmospheric Administration (NOAA): the Marine Resource Monitoring, Assessment, and Prediction (MARMAP) program and the Ecosystem Monitoring (EcoMon) program (Richardson et al. 2010). The MARMAP program operated from 1977 to 1987, and the EcoMon program has been active since 1992 (sample sizes collected by each program over time can be found in Figure S1). Both programs were designed to describe and assess changes in oceanography and planktonic community structure of the NEUS. Surveys were performed four to eight times per year over the continental shelf, spanning from Cape Hatteras, North Carolina, to Cape Sable, Nova Scotia (Richardson et al. 2010; Walsh et al. 2015). However, the programs have not necessarily completed all sampling as designed, which has resulted in some years with incomplete surveying. The programs' samples were taken throughout the year at both day and night. Deployments were performed with a 61 cm bongo net. Flowmeters equipped to the bongo nets were used to measure the volume of water filtered. Bongo nets were towed obliquely through the water column to within 5 m of the bottom, or a maximum of 200m (Richardson et al. 2010; Walsh et al. 2015).

The primary difference between the MARMAP and EcoMon programs is the mesh size of the bongo nets for ichthyoplankton sampling; the MARMAP program used 0.505 mm mesh, whereas the EcoMon uses a 0.333 mm mesh net (time series of samples by mesh size can be found in Figure S2). Discrepancy in mesh sizes used over time can cause concern over comparability due to prospective larval extrusion or avoidance (Schobernd et al. 2017). When evaluating larval extrusion considerations for various finfish species in the NEUS, Johnson and Morse (1992) did not find significant differences in larval yellowtail flounder catch between 0.333mm and 0.505mm meshes. While yellowtail flounder larvae were only found in one of the seven cruises conducted as part of the study, based on the results, the changes in mesh size over time were not considered to have a significant influence on detecting larvae present or estimating larval abundance of yellowtail flounder. This discrepancy over time does not apply to zooplankton sampling, as zooplankton samples were taken consistently with a 0.333 mm mesh net during both programs.

Zooplankton and ichthyoplankton specimens were identified to the lowest possible taxon (Kane 2008, Walsh et al. 2015). Abundances were standardized to number per 10 m^2 based on the proportion of the sample processed, the volume filtered by the nets, and the depths the nets sampled. Surface and bottom temperature and salinity were also measured concurrently, and CTD profiles conducted during the EcoMon Program. For further descriptions of the monitoring programs, please see Kane (2003) and Richardson et al. (2010).

Habitat Suitability Modeling

Plankton program samples were restricted to those that fell within US yellowtail flounder stock bounds (Figure 1). Analyses aimed to model yellowtail flounder

occurrence (presence/absence) and abundance (# larvae $10m^{-2}$). Yellowtail flounder have been observed in 10.5% of all ichthyoplankton samples collected over time. Larval presence by month is greatest from April through August, with approximately 2-3% of all other larval presence occurring in other months. Given this, habitat suitability models only included data from April through August (Figures S3 and S4). Larval sizes observed in the survey ranged from 0.5mm to 117.2mm, though nearly 98% of all larvae observed were between egg hatch (2.1mm) and metamorphosis (14.0mm) size thresholds, and thus were all considered planktonic larvae available to the bongo nets (Figure S5).

Several covariates were evaluated for modeling larval yellowtail flounder. Concurrent physical oceanographic sampling from the EcoMon and MARMAP surveys were examined, specifically surface and bottom temperature and salinity measurements. Water column stratification was also evaluated by calculating the difference between bottom and surface water densities, with water density (kg/m^3) calculated using the 'sw_dens' function in R package 'marelec'. Zooplankton abundances were also evaluated to understand the reliance of larvae on zooplankton as prey, as previous recruitment regimes for groundfish (including yellowtail flounder) recruitment in the region have been associated with patterns in the zooplankton community (Perretti et al. 2017). Without larval diet information available to test species-specific dietary reliance, copepod densities were based on size spectrum of taxa (Ecosystem Assessment Program 2011; Perretti et al. 2017). Copepod *Calanus finmarchicus* was tested in modeling as an indicator of changes in large sized zooplankton species in the community. As an indicated for small bodied copepod taxa, the sum of species *Pseudocalanus* spp.*, Centropages typicus, Centropages hamatus,* and *Temora longicornis* were tested in modeling. Large scale climatic forcing was evaluated through testing of the North Atlantic Oscillation (NAO) index. The NAO has shown to influence various aspects of the marine ecosystem within the NEUS, specifically oceanography and lower trophic level productivity, and subsequently higher trophic levels. The NAO has previously been linked to yellowtail flounder recruitment in the SNEMA region (Brodziak and O'Brien 2005; Sullivan et al. 2005). Annual NAO winter (Dec-Mar) indices were obtained from Hurrell (2003). Indices were lagged two years based on reported lag times with the NAO and other ecosystem processes within the NEUS (MERCINA 2001; MERCINA 2004), and previous work indicating a two year lag was strongest in environmental-recruitment analyses (Brodziak et al. 2005). When evaluating covariates for modeling, cross correlations and variance inflation factors between variables were evaluated to minimize probability of model overfitting. From this examination, bottom temperature and salinity were removed from model fitting exercises.

Generalized additive models (GAMs) were implemented to describe the relationships between larval abundance and the environment. GAMs use smooth

additive functions, resulting in curvature or splines in the predictions (Hastie and Tibshirani 1986, Wood 2006). Two statistical frameworks were used within the GAMs to model larval abundance. The first modeled presence/absence, or occurrence, of yellowtail flounder larvae using a binomial error distribution. The second modeled abundance with a Tweedie error distribution. The goal of using these two frameworks was to determine if the high zero-inflation in the dependent variable influenced final results in habitat suitability modeling. Within the GAMs, the gamma parameter was fixed to 1.4 to reduce model overfitting, as recommended by Wood (2006). Final models for predicting larvae (presence/absence and abundance) included the following variables:

$$Larvae_y \sim s(surface\ temperature_y)+s(surface\ salinity_y)+s(depth_y)+s(Calanus\ finmarchicus_y)+s(small\ copepods_y)+s(stratification_y)+(Winter\ NAO_{y-2})+Stock\ Unit$$

where ‘s’ represents instances where variables were modeled with smooth additive functions. Variables modeled with smoothing functions were unconstrained in knots, though a sensitivity on fixing the number of knots for smooth functions was conducted to evaluate model diagnostics. Stock unit (CCGOM, GB, or SNEMA) was incorporated as a factor variable to acknowledge the time series average difference in the biological population unit sizes (e.g. spawning stock biomass). However, this variable was not modeled with an interaction term and did not capture dynamic changes over time (e.g. Year:Stock) or with other modeled covariates (e.g. surface temperature:Stock). The mesh size was not included in the models; however occurence models were also run on just MARMAP and EcoMon data as a sensitivity to see if the relationships between occurrence and the environment, and model performances, were different. Lastly, the model predictions from the abundance model using a Tweedie distribution and a Hurdle model framework (presence/absence and abundance-only GAMs developed and predictions multiplied) were compared to determine if predictions assuming different approaches in statistical model fitting of abundance data resulted in substantially different predictions.

Final GAMs were used to predict probability of occurence (binomial GAM) and abundance (Tweedie GAM) over all samples. Predictions were then spatially interpolated over a 0.1°grid encompassing the three stock units of the NEUS. Spatial correlation in probability of occurrence and abundance were evaluated through producing variograms; however, spatial correlation for these variables were weak or nonexistent, with variograms either not fitted or deemed uninformative in kriging predictions spatially. As such, grid predictions were carried out using inverse distance weighting of the GAM predictions using a power of 2.

Grid cell values of abundance and probability of occurrence were averaged by year and stock unit. These values, and the equivalent Z-scores, were used to represent annual indices of habitat suitability. Annual habitat index values were only included as part of the time series if there was adequate spatial coverage for the given stock, which

resulted in some years' predictions not being included in the indices (Table1). Habitat suitability indices using occurrence and abundance predictions were compared by stock, as well as the influence of inverse distance weighting assumptions (powers 1, 2, 3) on the final habitat suitability indices. SNEMA habitat suitability indices were compared to larval abundance indices (Richardson et al. 2014), which have been used in the SNEMA stock assessment model to inform recruitment (NEFSC 2022).

Results

Habitat Models

All variables were found to be significant in predicting yellowtail flounder larval occurrence and abundance, each GAM indicating similar relationships between larvae and the environment (Figures 2 and 3). Larval occurrence and abundance were generally greatest at temperatures between approximately 5-15°C, depths shallower than 100m, higher abundances of smaller sized copepods, and greater stratification (Figures 2 and 3). Relationships between other significant variables indicated more complex relationships or driven by outliers in the dataset, such as for surface salinity, *Calanus finmarchicus*, and the Winter NAO (Figure 2). Occurrence was highest for GB, followed by SNEMA and then CCGOM. Results from the abundance GAM indicated similar patterns as the occurrence GAM, with the most pronounced differences being a more domed depth preferential range between 0-100m, more pronounced relationship profile with small copepods, and more neutral response to water column stratification in the abundance GAM than the occurrence GAM (Figure 3). The occurrence model explained 31.0% of the deviance, and the abundance model explained 51.2% of the deviance (Table 2).

Sensitivity models that tested the influence of setting the number of knots for independent variables resulted in reduced model fitness (Table 2). Visual inspection of the relationship between covariates and larvae in these constrained models allowed for further understanding the degree of model overfitting to data points and better theorize the functional relationship between the variables (Figure S6). When building models specific to plankton programs (i.e. MARMAP and EcoMon individually), the models explained slightly more deviance than modeling all data at once (Table 2). However, all data were modeled together in order to analyze the entire time series at once with comparable predictions over time. The Tweedie and Hurdle abundance model predictions were strongly correlated (R^2=0.78, p-value<0.001), and thus the Tweedie abundance model was used for developing indices.

Spatial Predictions and Habitat Suitability Indices

Interpolated predictions of larval occurrence and abundance indicated interannual variability by stock unit and the larger NEUS (Figure 4). The influence of inverse distance weighting assumption (powers 1, 2, 3) on the occurrence habitat suitability indices was small, as the correlations between indices were strong (idw

powers 2 and 3: R^2=0.98; idw powers 1 and 2: R^2=0.89). Habitat suitability indices by model type (occurrence vs. abundance) were also strongly correlated (Figure 5), and thus only the abundance-derived indices are presented in the main text (figures for occurrence models are in Figures S7 and S8). Over time, habitat suitability appeared to be greatest for the GB and SNEMA stocks than in CCGOM (Figures 6 and 7). While indices were variable over time, some trends did emerge. For both index calculation types, habitat suitability appeared to increase from the late 1970s through the mid-late 1980s, but from the 2000s through the 2010s, habitat suitability declined. When comparing the SNEMA habitat suitability index (abundance z-score) to the larval abundance index used to inform recruitment in previous stock assessment models, the correlation was weak, but significant (R^2=0.23, p-value=0.04, Figure 8).

Discussion

The correspondence between yellowtail flounder larvae and oceanography provides another example of environmental drivers on larval fish (McManus et al. 2018; Morson et al. 2019; Taxton et al. 2020; McManus et al. 2022; Weisberg et al. 2024) but also specifically to yellowtail flounder (Perretti et al. 2017; du Pontavice et al. 2022; Kittel et al. 2024). However, the weak correlation between larval abundance and habitat suitability for SNEMA suggests that the environmental habitat conditions may not be the greatest determinant in SNEMA larval production. Although the information was informative regarding prospective habitat requirements for larval yellowtail flounder and offers a mechanism for environmental effects on yellowtail flounder recruitment, the Working Group elected to not use the habitat indices as environmental covariates within the stocks' assessment models at this time. Future larval habitat suitability modeling could be include testing different methodologies for spatial predictions and forecasting model covariates to allow for future predictions of larval habitat. Comparing larval abundance indices the corresponding habitat indices for the other stocks (CCGOM and GB) would also be useful to understand whether the correspondence varies by stock.

Literature Cited

Brodziak J and O'Brien L. 2005. Do environmental factors affect recruits per spawner anomalies of New England groundfish? ICES Journal of Marine Science 62: 1394–1407.

du Pontavice, H., Miller, T.J., Stock, B.C., Chen, Z., Saba, V.S. 2022. Ocean model-based covariates improve a marine fish stock assessment when observations are limited, ICES Journal of Marine Science 79(4): 1259–1273.

Ecosystem Assessment Program. 2011. Ecosystem status report for the Northeast U.S. continental shelf Large Marine Ecosystem. US Department of Commerce, Woods Hole, MA

Hastie, T., & Tibshirani, R. 1986. Generalized additive models. Statistical Science, 1: 297–310.

Johnson, D. L., & Morse, W. W. 1994. Net extrusion of larval fish: Correction factors for 0.333 mm versus 0.505 mm mesh bongo nets. NAFO Scientific Council Studies, 20, 85–92.

Kane, J. 2003. Spatial and temporal abundance patterns for late stage copepodites of *Metridia lucens* (Copepoda: Calanoida) in the US northeast continental shelf ecosystem. Journal of Plankton Research, 25(2), 151–167.

Kittel, J., Cadrin, S., McManus, C., Hansell, A., Dolan, T., Legault, C., Adams, C., Alade, L., du Pontavice, H., Kerr, L., Behan, J., Large, S., Tyrell, A., Schaffer, S. 2024. TOR1: Ecosystem and Climate Influences. Working Paper Submitted as part of the Yellowtail Flounder Research Track Stock Assessment. 13pp.

McManus, M.C., Hare, J.A., Richardson, D.E., and Collie, J.S. 2018. Tracking shifts in Atlantic mackerel (*Scomber scombrus*) larval habitat suitability on the northeast U.S. Continental Shelf. Fisheries Oceanography 27:49–62.

McManus MC, Langan JA, Bell RJ, Collie JS, Klein-MacPhee G, Scherer MD, Balouskus RG. 2021. Spatiotemporal patterns in early life stage winter flounder *Pseudopleuronectes americanus* highlight phenology changes and habitat dependencies. Mar Ecol Prog Ser 677:161-175.

MERCINA. 2001.Oceanographic responses to climate in the northwest Atlantic. Oceanography,14:76–82.

MERCINA. 2004.Supply-side ecology and the response of zooplankton to climate-driven changes in North Atlantic ocean circulation. Oceanography,17:60–71.

Morson JM, Grothues T, Able KW. 2019. Change in larval fish assemblage in a USA east coast estuary estimated from twenty-six years of fixed weekly sampling. PLOS ONE 14(11): e0225526.

Hurrell (2003). NAO Index Data provided by the Climate Analysis Section, NCAR, Boulder, USA. Accessed 1 August 2023.

Perretti CT, Fogarty MJ, Friedland KD, Hare JA and others (2017) Regime shifts in fish recruitment on the Northeast US Continental Shelf. Mar Ecol Prog Ser 574:1-11.

Richardson, D. E., Hare, J. A., Overholtz, W. J., & Johnson, D. L. (2010). Development of long-term larval indices for Atlantic herring (Clupea harengus) on the northeast US continental shelf. ICES Journal of Marine Science: Journal du Conseil, 67, 617–627.

Richardson, D.E., Marancik, K., and Walsh, H. 2014. A larval index for Georges Bank yellowtail flounder with comparisons of relative larval production between yellowtail flounder stock areas. Transboundary Resources Assessment Committee Document de travail 2014/19 Working Paper 2014/19. 11p.

Schobernd, CM, McManus, MC, Lyczkowski-Shultz, Bacheler, NM, and Drass, DM. 2018. Extrusion of fish larvae from SEAMAP plankton sampling nets: a comparison between 0.333-mm and 0.202-mm mesh nets. Fishery Bulletin. 116: 240-253.

Sullivan MC, Cowen RK, Steves BP. 2005. Evidence for atmosphere–ocean forcing of yellowtail flounder (Limanda ferruginea) recruitment in the Middle Atlantic Bight. Fisheries Oceanography 14: 386-399.

Thaxton WC, Taylor JC, Asch RG (2020) Climate-associated trends and variability in ichthyoplankton phenology from the longest continuous larval fish time series on the east coast of the United States. Mar Ecol Prog Ser 650:269-287.

Walsh, H. J., Richardson, D. E., Marancik, K. E., & Hare, J. A. (2015). Long-Term Changes in the Distributions of Larval and Adult Fish in the Northeast U.S. Shelf Ecosystem. PLoS ONE, 10, e0137382.

Weisberg, S.J., Roberts, S.M., Gruenburg, L.K., Schwemmer, T.G., Menz, T., Fenwick, I.F., Nye, J.A. and Asch, R.G., 2024. Gulf Stream intrusions associated with extreme seasonal fluctuations among larval fishes. Marine Ecology Progress Series, 739:157-172.

Wood, S. N. (2006). Generalized additive models: An introduction with R. Boca Raton, Florida: Chapman and Hall/CRC Press.

Table 1. Gantt table indicating years of which data were deemed available for use in predicting habitat suitability based on sample coverage. Red indicates years with data used.

Year	CCGOM	GB	SNE
1977			
1978			
1979			
1980			
1981			
1982			
1983			
1984			
1985			
1986			
1987			
1988			
1989			
1990			
1991			
1992			
1993			
1994			
1995			
1996			
1997			
1998			
1999			
2000			
2001			
2002			
2003			
2004			
2005			
2006			
2007			
2008			
2009			
2010			
2011			
2012			
2013			
2014			
2015			

Table 2. Variance explained for each base model and selected sensitivities

Model	Deviance Explained
Base	
Occurrence	31.0%
Tweedie	51.2%
Knots	
Occurrence, k=3	24.9%
Occurrence, k=5	27.5%
Plankton Program	
Occurrence, MARMAP only	37.6%
Occurrence, EcoMon only	32.4%

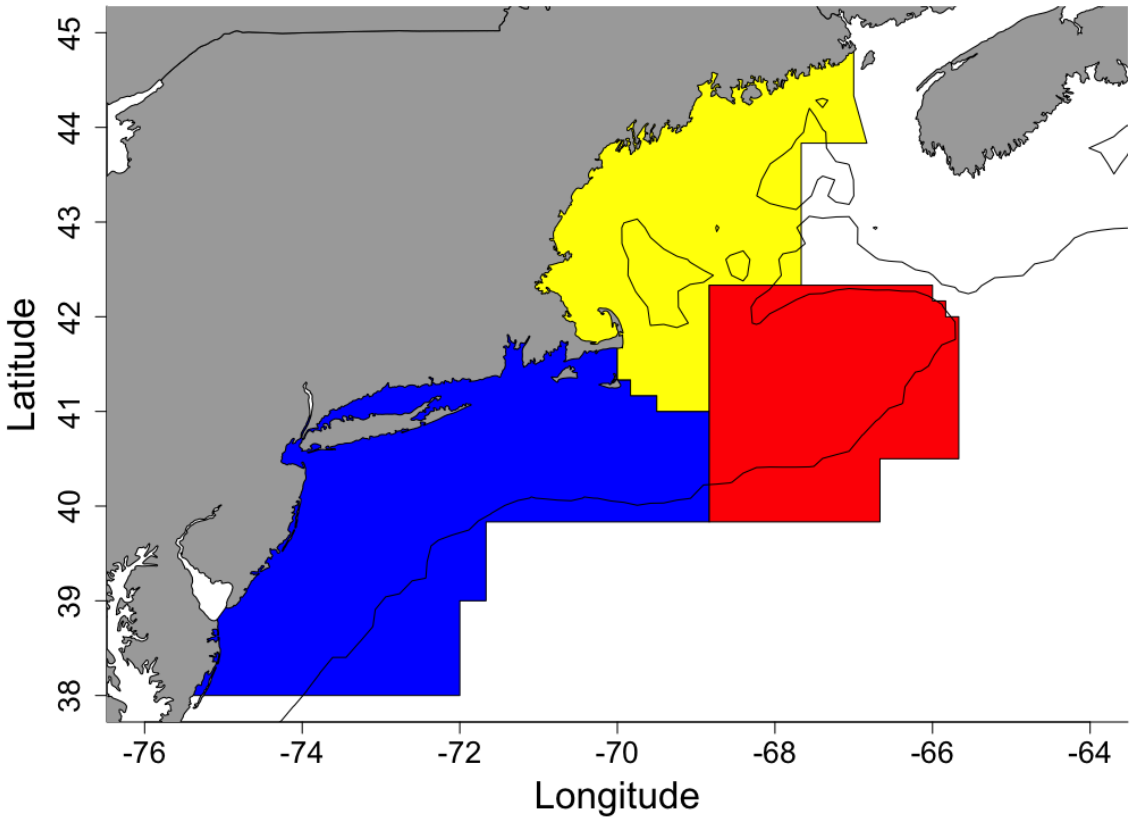

Figure 1. Yellowtail flounder U.S. stock units: SNE/MA (blue), GB (red), CCGOM (green). Dark line represents the 200m bathymetry contour.

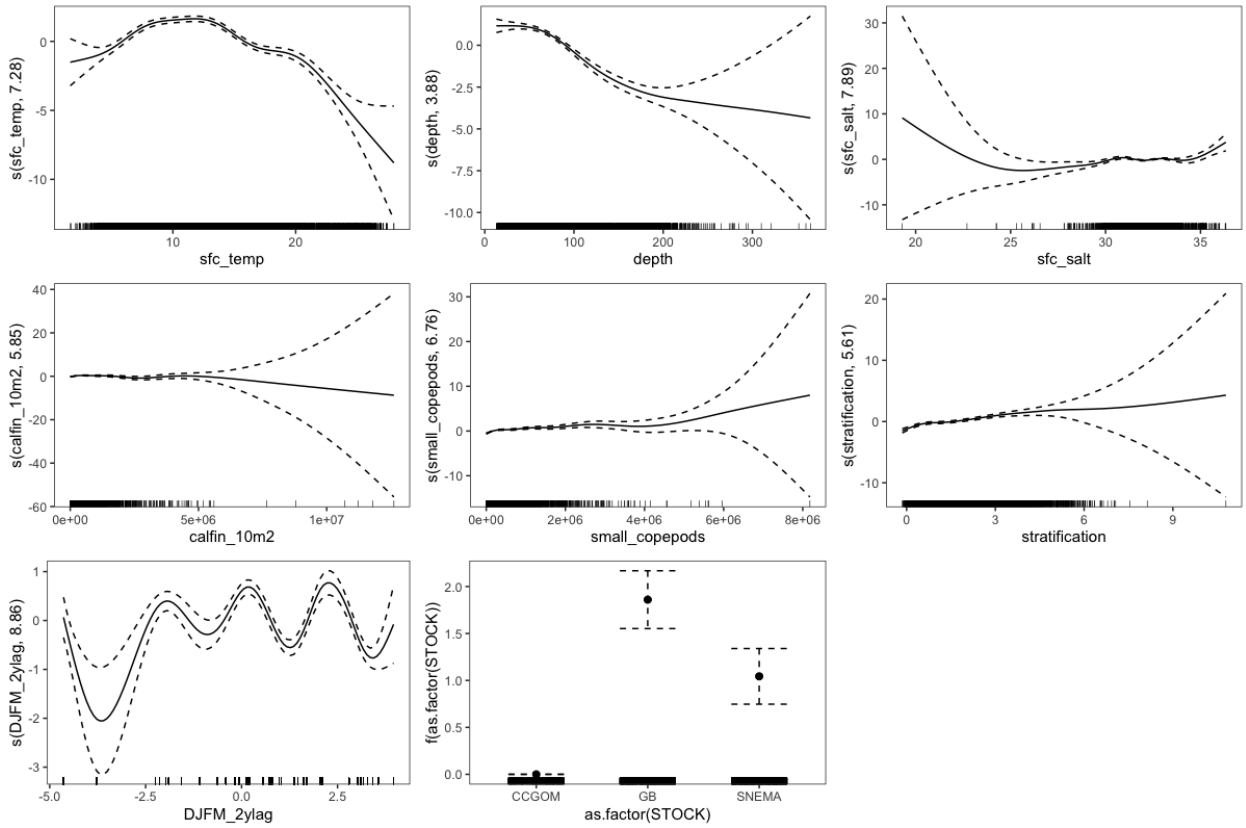

Figure 2. Covariates' relationship to yellowtail flounder larvae in occurrence (binomial) GAM.

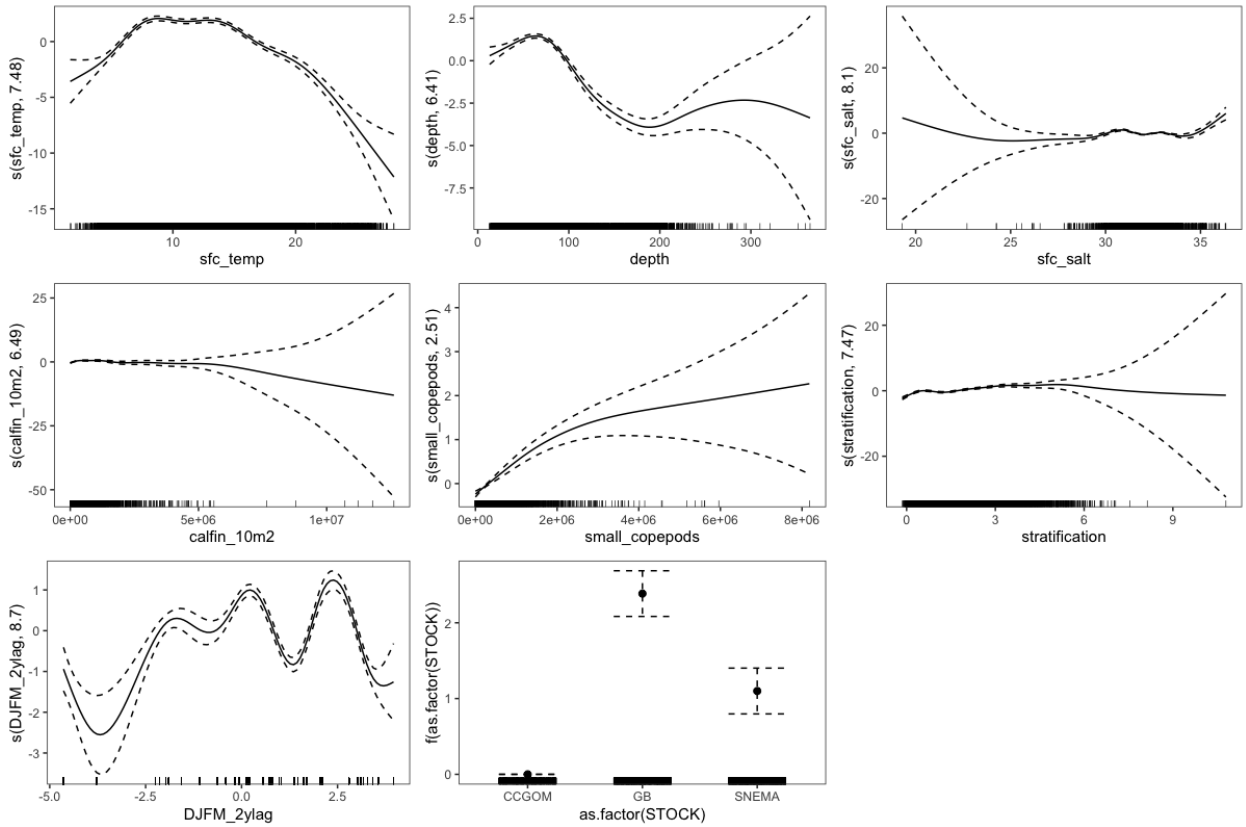

Figure 3. Covariates' relationship to yellowtail flounder larvae in abundance (Tweedie) GAM.

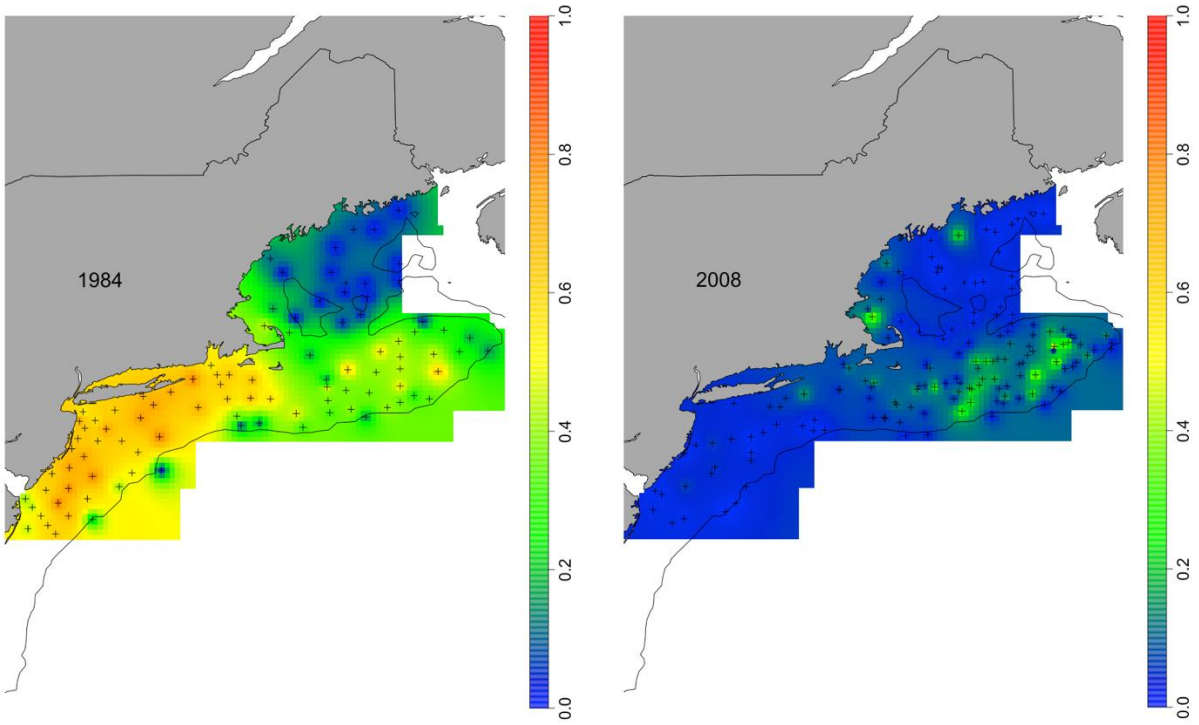

Figure 4. Spatially interpolated (idw) larval occurrence in stock units for two contrasting years of high (1984, left) and low (2008, right) occurrence. The solid line within the NEUS is the 200m bathymetry contour. Cross marks represent sample locations specific to each year.

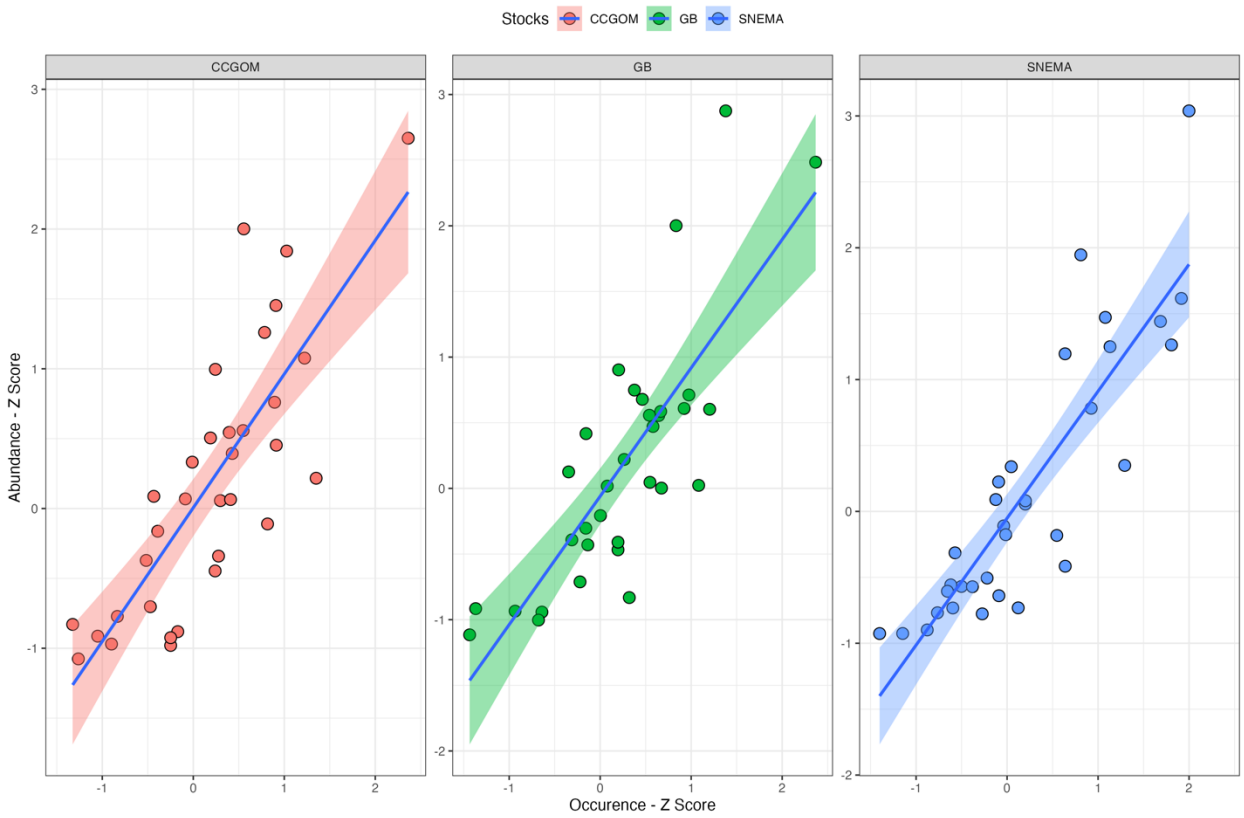

Figure 5. Correlation between Z score habitat suitability indices by model type (Occurrence and Abundance) by stock.

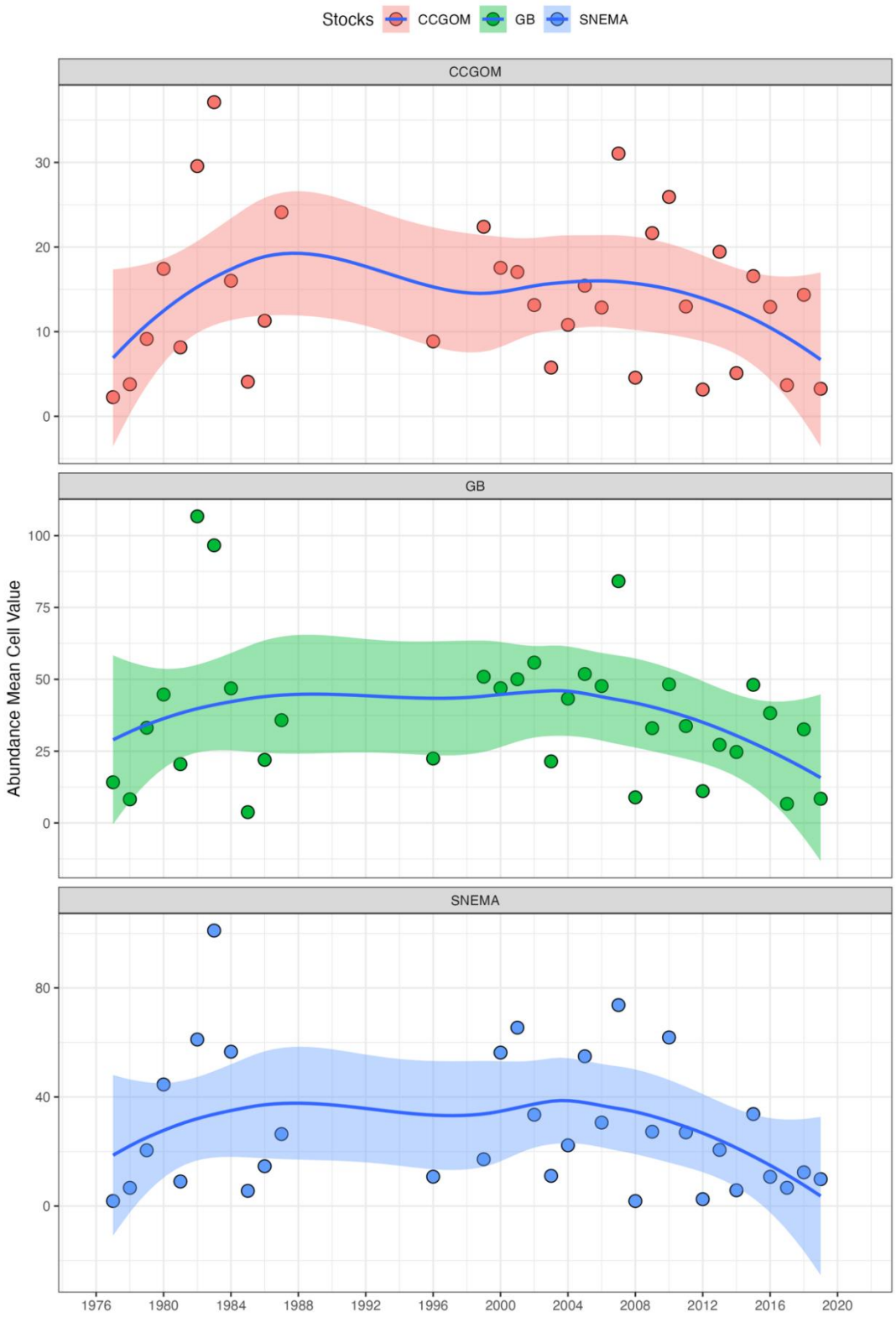

Figure 6. Habitat suitability index of mean annual values by stock for abundance predictions.

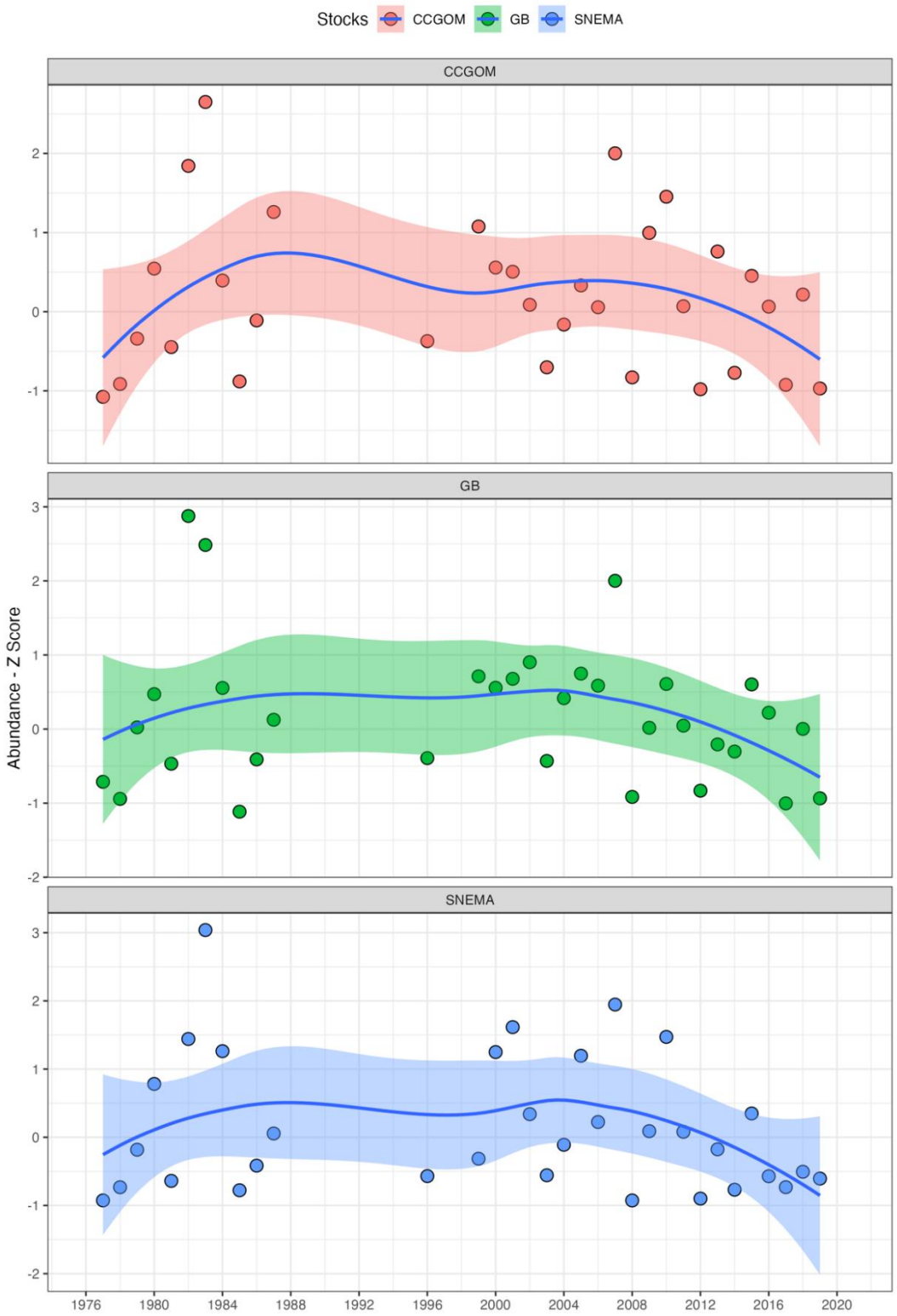

Figure 7. Habitat suitability index of mean annual values by stock for abundance predictions expressed as Z-scores.

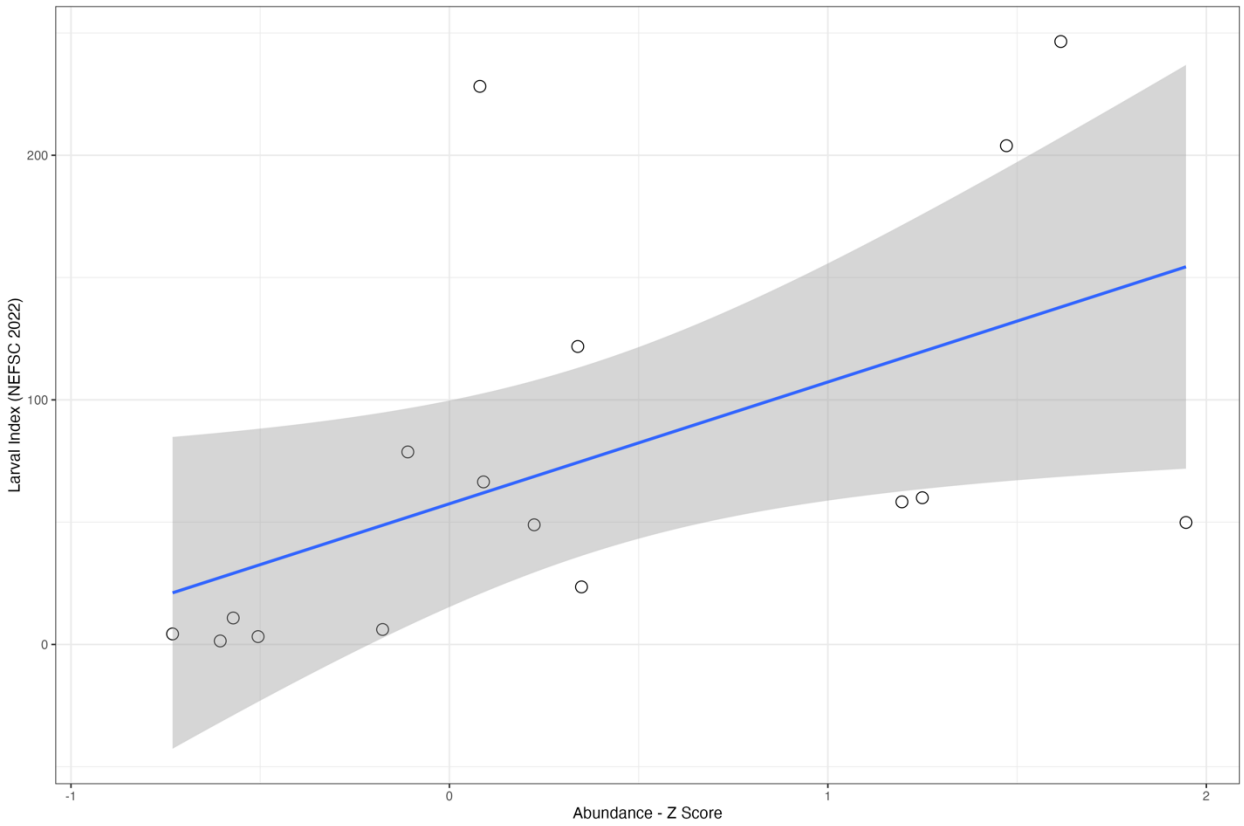

Figure 8. Comparison of the SNEMA Habitat Suitability Index (Z Score) and the Larval Index used for the stock assessment model as used in NEFSC (2022). Blue line and gray polygon represent the linear fit and standard error (R^2=0.23, p-value=0.04).

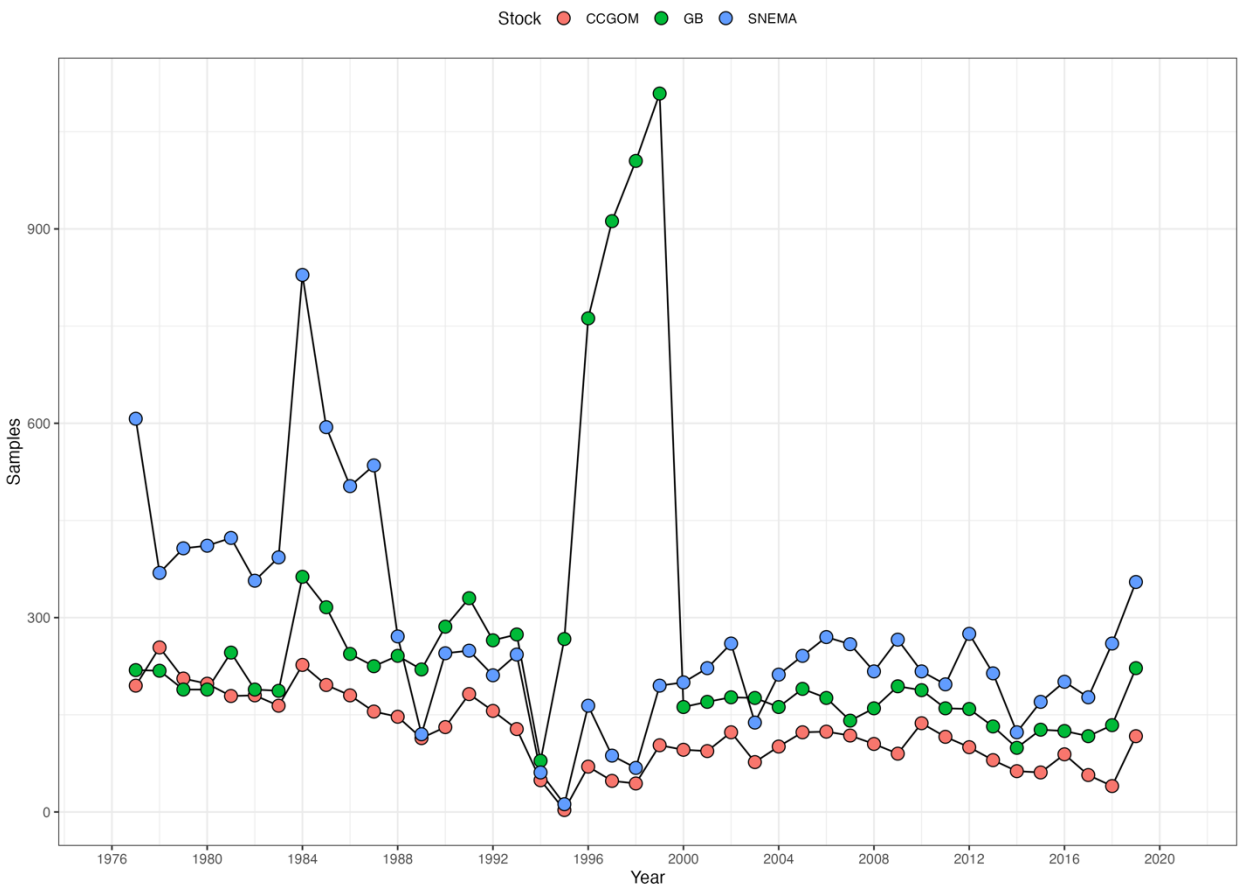

Figure S1. Number of samples from the MARMAP and EcoMon programs available for habitat suitability modeling by stock unit and year.

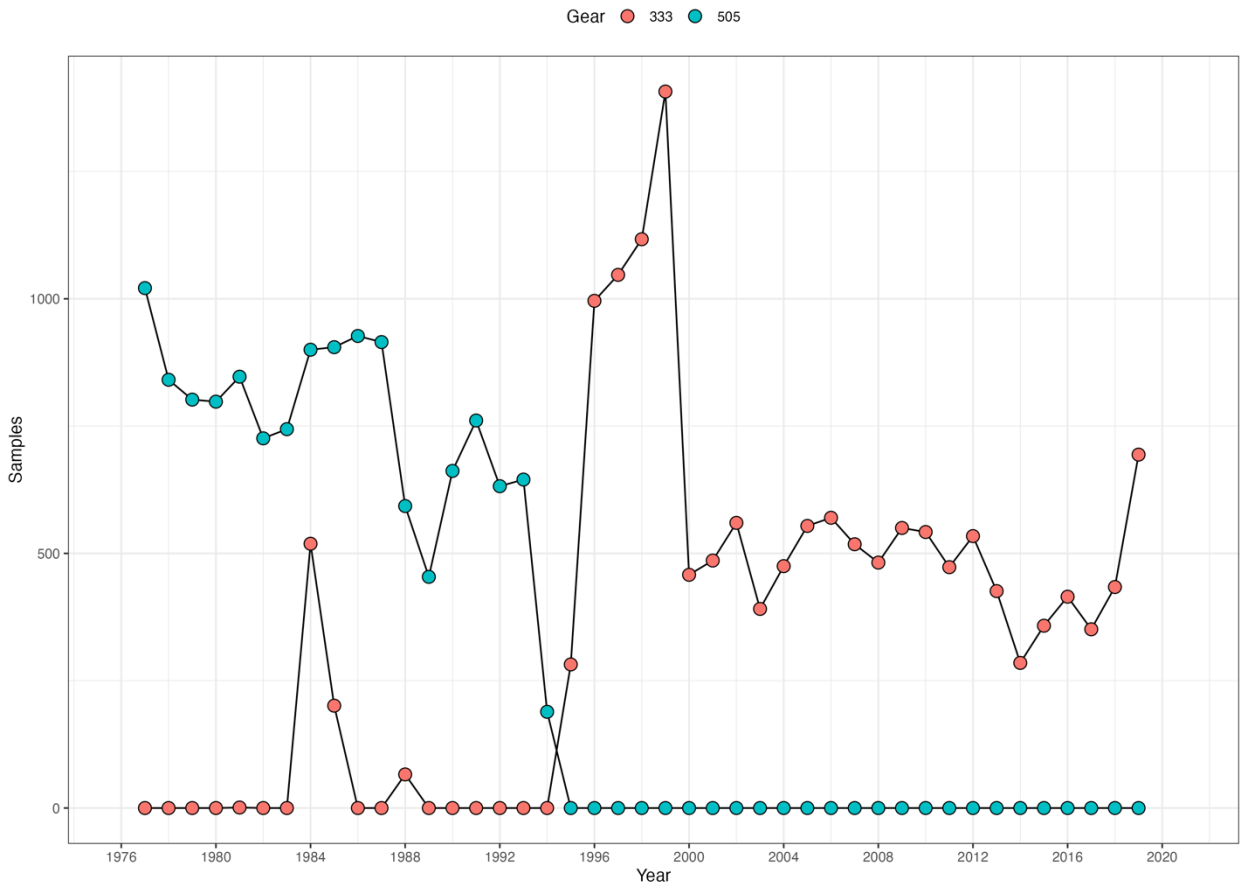

Figure S2. Number of samples collected from the larval surveys over time with 0.333mm and 0.505mm mesh bongo nets.

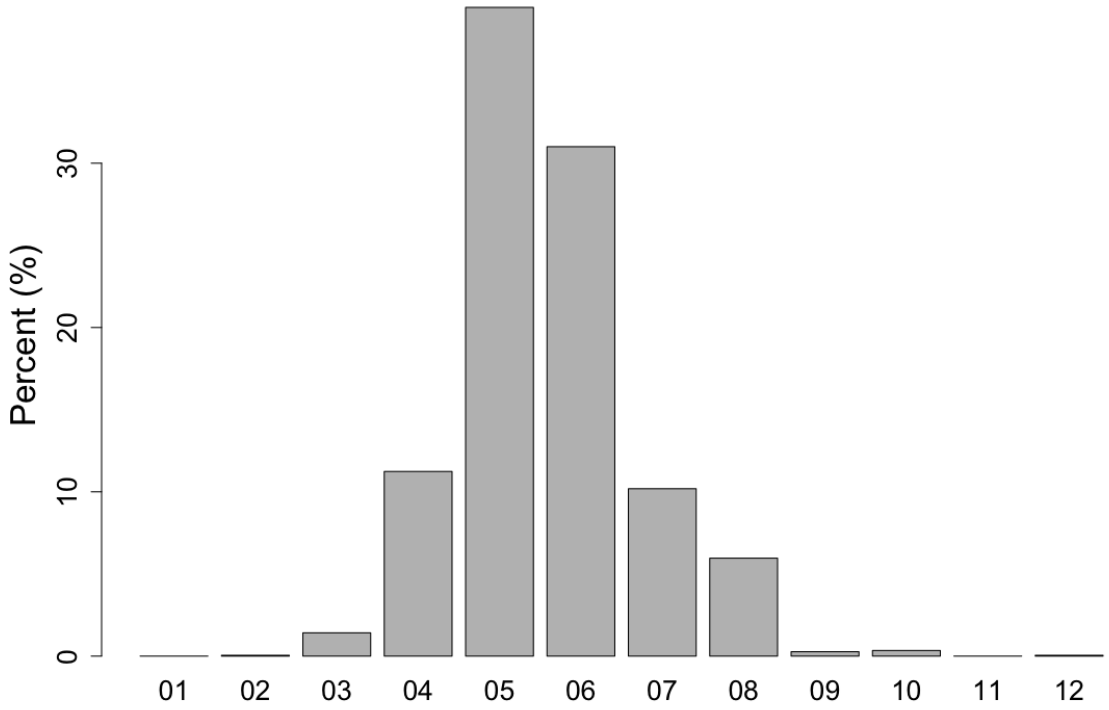

Figure S3. Percent of samples with larval yellowtail flounder by month across all years.

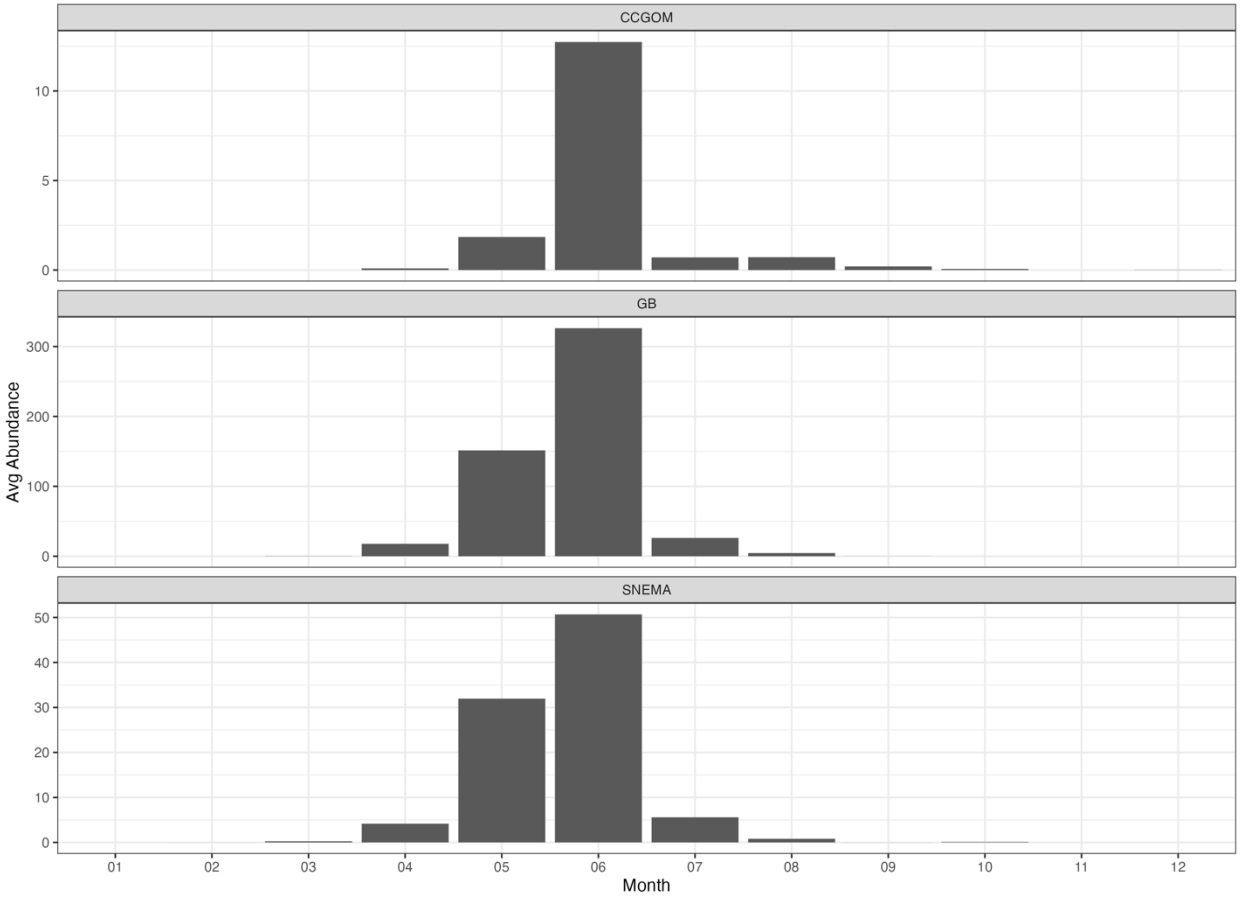

Figure S4. Average larval abundance by month and stock over the time series.

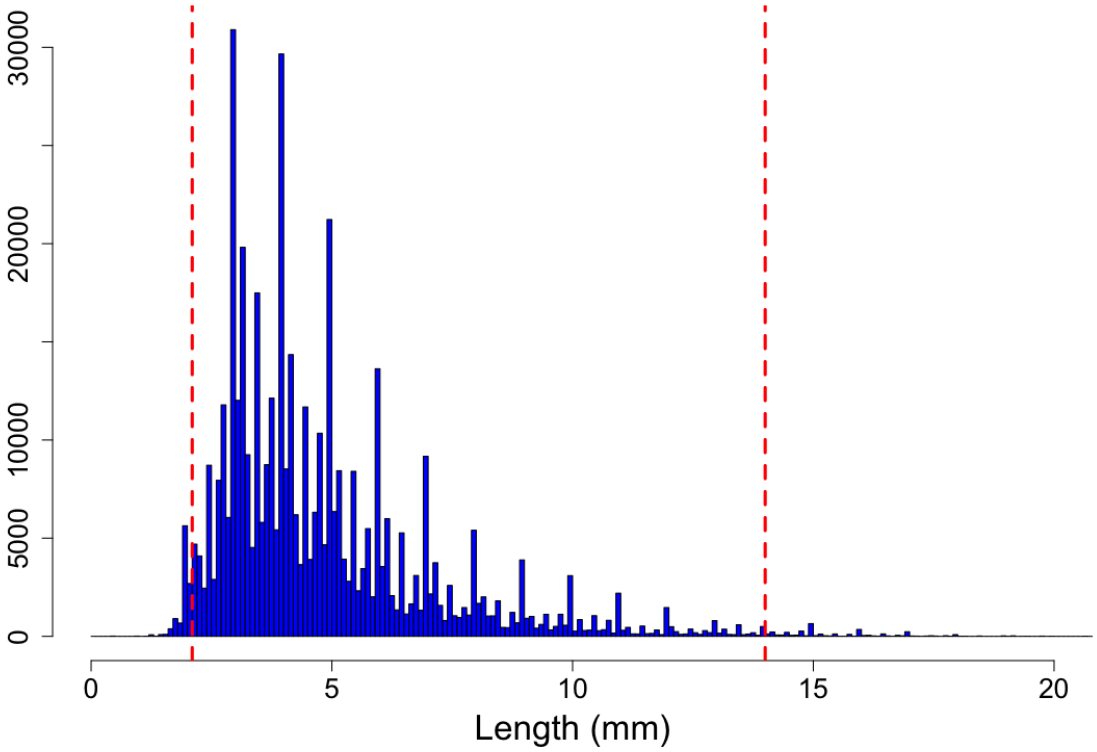

Figure S5. Distribution of larval yellowtail founder larvae by size. Red dashed lines represent sizes at which eggs hatch (2.1mm) and larvae metamorphose (14.0mm).

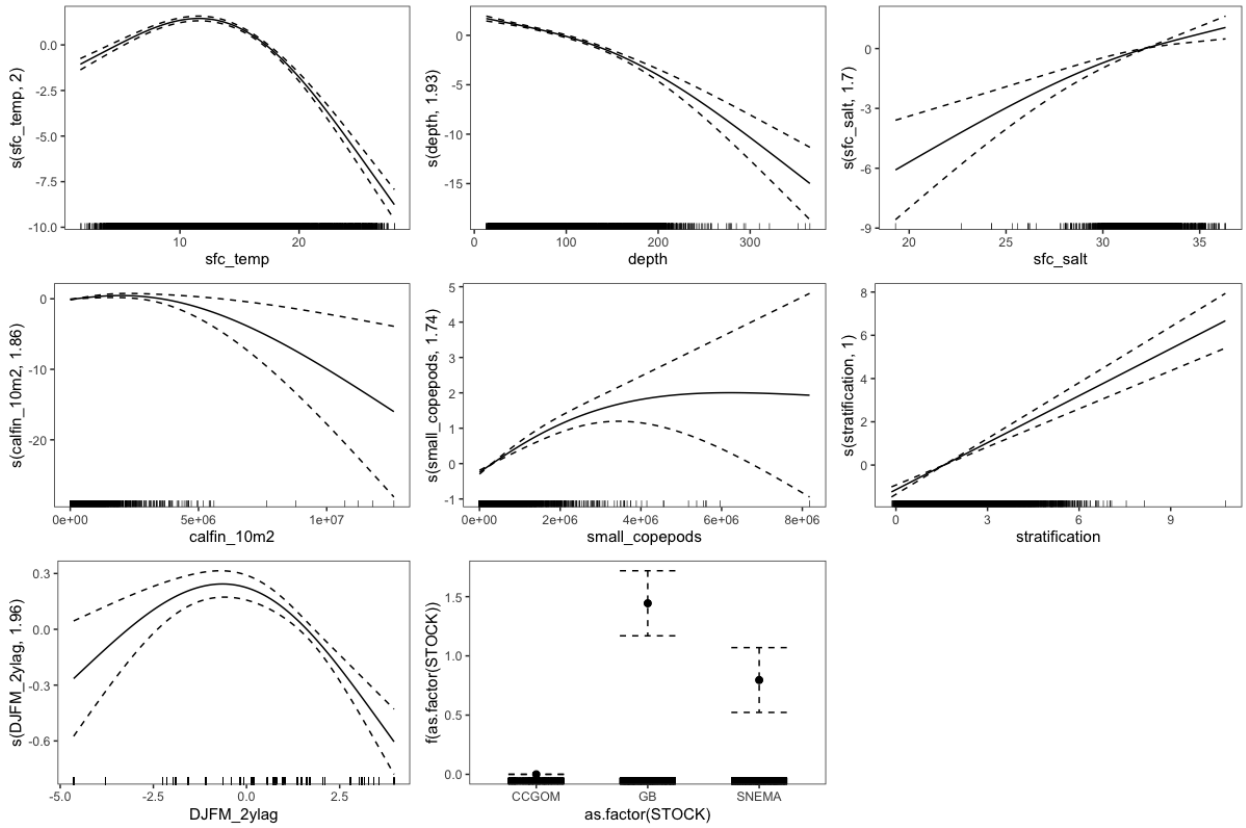

Figure S6. Figure 2. Covariates' relationship to yellowtail flounder larvae in occurrence (binomial) GAM when the continuous variables' knots are set to 3.

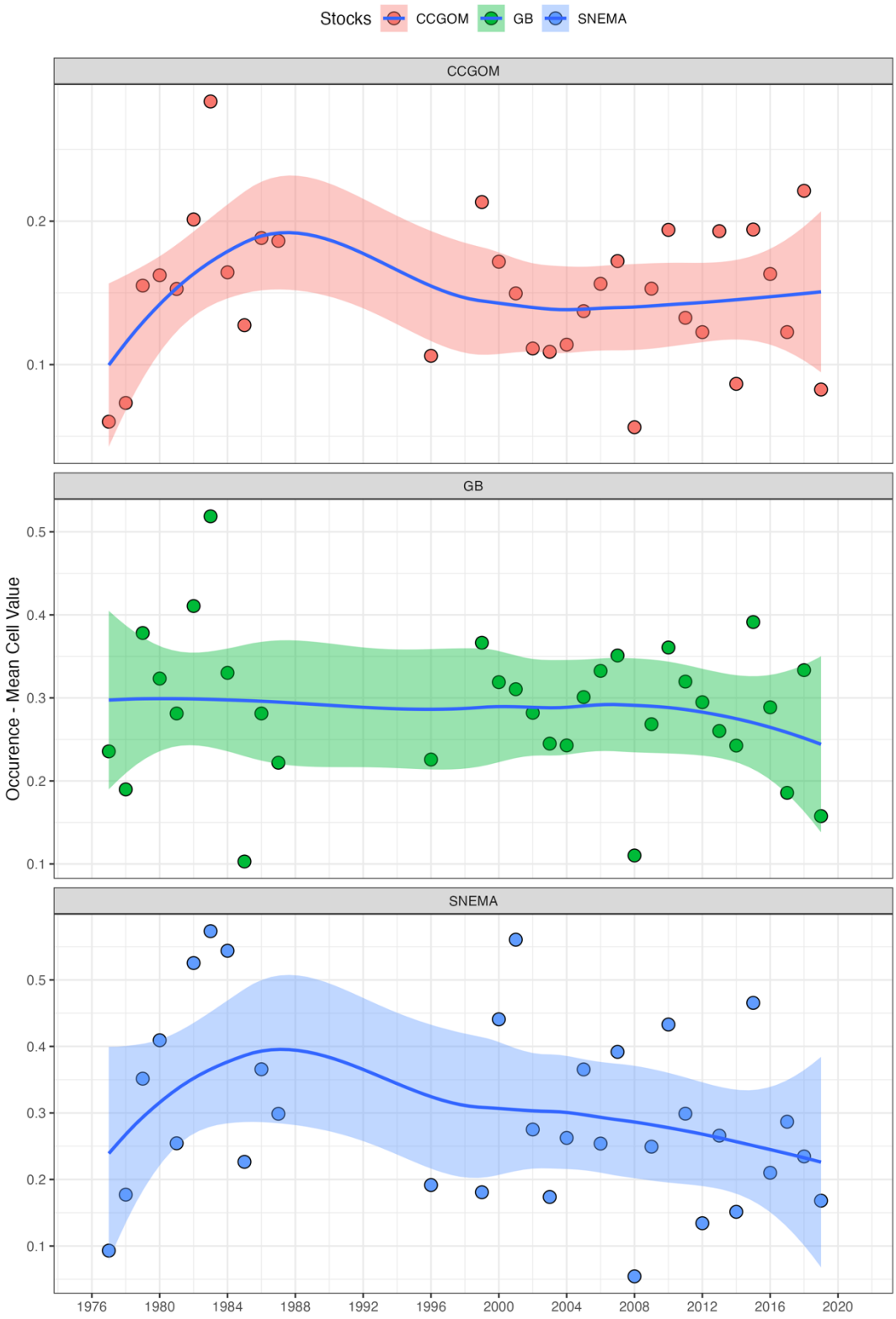

Figure S7. Habitat suitability index of mean annual values by stock for occurrence predictions. Fitted lines represents loess fits to the indices with standard errors.

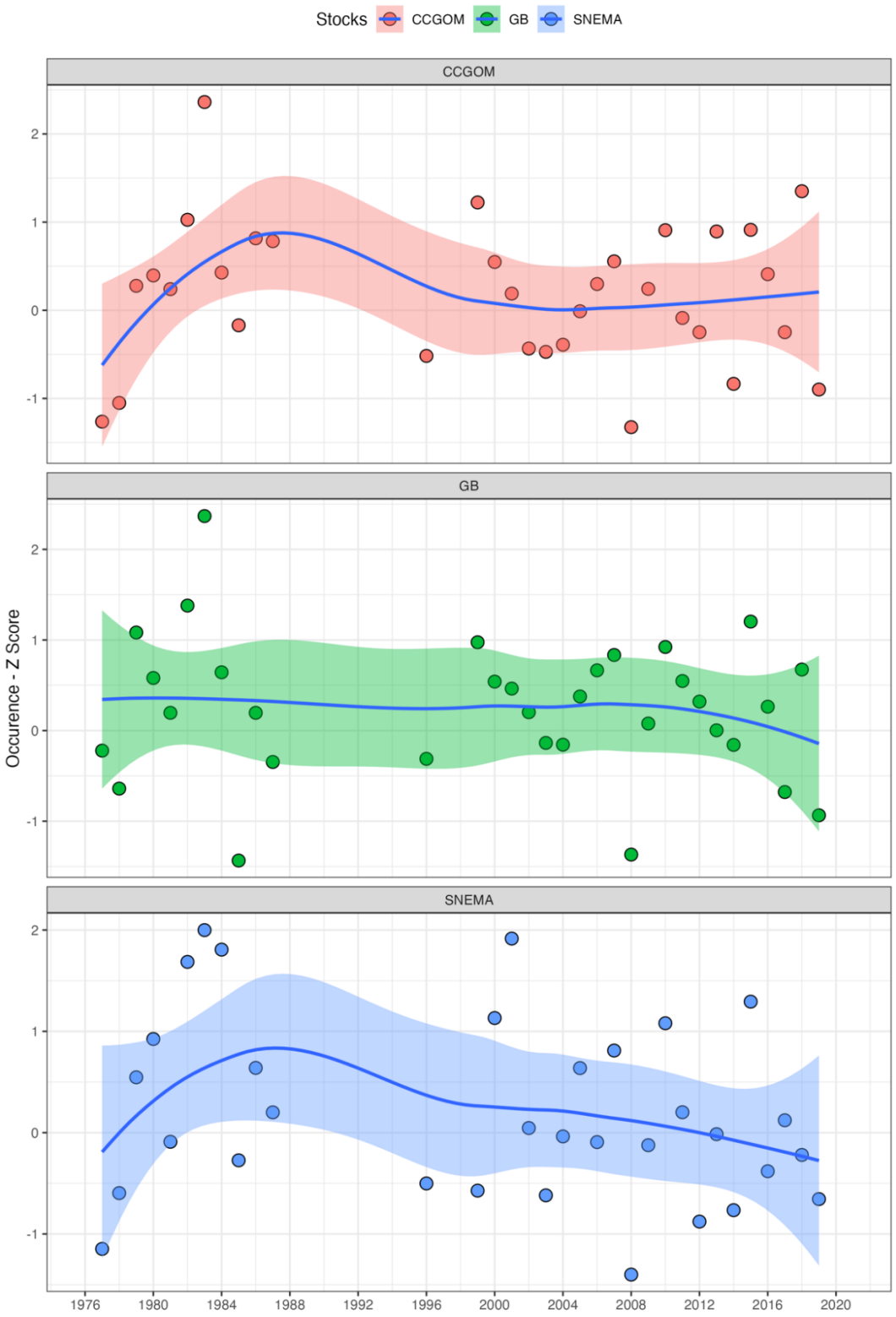

Figure S8. Habitat suitability index of mean annual values by stock for occurrence predictions expressed as Z-scores.